Search for the Familon via $B^\pm \to \pi^\pm X^0$, $B^\pm \to K^\pm X^0$, and $B^0 \to K_S^0 X^0$ Decays

R. Ammar,[1] A. Bean,[1] D. Besson,[1] X. Zhao,[1] S. Anderson,[2] V. V. Frolov,[2] Y. Kubota,[2] S. J. Lee,[2] R. Poling,[2] A. Smith,[2] C. J. Stepaniak,[2] J. Urheim,[2] S. Ahmed,[3] M. S. Alam,[3] S. B. Athar,[3] L. Jian,[3] L. Ling,[3] M. Saleem,[3] S. Timm,[3] F. Wappler,[3] A. Anastassov,[4] E. Eckhart,[4] K. K. Gan,[4] C. Gwon,[4] T. Hart,[4] K. Honscheid,[4] D. Hufnagel,[4] H. Kagan,[4] R. Kass,[4] T. K. Pedlar,[4] J. B. Thayer,[4] E. von Toerne,[4] M. M. Zoeller,[4] S. J. Richichi,[5] H. Severini,[5] P. Skubic,[5] A. Undrus,[5] V. Savinov,[6] S. Chen,[7] J. W. Hinson,[7] J. Lee,[7] D. H. Miller,[7] V. Pavlunin,[7] E. I. Shibata,[7] I. P. J. Shipsey,[7] D. Cronin-Hennessy,[8] A. L. Lyon,[8] E. H. Thorndike,[8] T. E. Coan,[9] V. Fadeyev,[9] Y. S. Gao,[9] Y. Maravin,[9] I. Narsky,[9] R. Stroynowski,[9] J. Ye,[9] T. Wlodek,[9] M. Artuso,[10] K. Benslama,[10] C. Boulahouache,[10] K. Bukin,[10] E. Dambasuren,[10] G. Majumder,[10] R. Mountain,[10] T. Skwarnicki,[10] S. Stone,[10] J. C. Wang,[10] A. Wolf,[10] S. Kopp,[11] M. Kostin,[11] A. H. Mahmood,[12] S. E. Csorna,[13] I. Danko,[13] K. W. McLean,[13] Z. Xu,[13] R. Godang,[14] G. Bonvicini,[15] D. Cinabro,[15] M. Dubrovin,[15] S. McGee,[15] A. Bornheim,[16] E. Lipeles,[16] S. P. Pappas,[16] A. Shapiro,[16] W. M. Sun,[16] A. J. Weinstein,[16] D. E. Jaffe,[17] R. Mahapatra,[17] G. Masek,[17] H. P. Paar,[17] D. M. Asner,[18] A. Eppich,[18] T. S. Hill,[18] R. J. Morrison,[18] R. A. Briere,[19] G. P. Chen,[19] T. Ferguson,[19] H. Vogel,[19] J. P. Alexander,[20] C. Bebek,[20] B. E. Berger,[20] K. Berkelman,[20] F. Blanc,[20] V. Boisvert,[20] D. G. Cassel,[20] P. S. Drell,[20] J. E. Duboscq,[20] K. M. Ecklund,[20] R. Ehrlich,[20] P. Gaidarev,[20] L. Gibbons,[20] B. Gittelman,[20] S. W. Gray,[20] D. L. Hartill,[20] B. K. Heltsley,[20] L. Hsu,[20] C. D. Jones,[20] J. Kandaswamy,[20] D. L. Kreinick,[20] M. Lohner,[20] A. Magerkurth,[20] H. Mahlke-Krüger,[20] T. O. Meyer,[20] N. B. Mistry,[20] E. Nordberg,[20] M. Palmer,[20] J. R. Patterson,[20] D. Peterson,[20] D. Riley,[20] A. Romano,[20] H. Schwarthoff,[20] J. G. Thayer,[20] D. Urner,[20] B. Valant-Spaight,[20] G. Viehhauser,[20] A. Warburton,[20] P. Avery,[21] C. Prescott,[21] A. I. Rubiera,[21] H. Stoeck,[21] J. Yelton,[21] G. Brandenburg,[22] A. Ershov,[22] D. Y.-J. Kim,[22] R. Wilson,[22] B. I. Eisenstein,[23] J. Ernst,[23] G. E. Gladding,[23] G. D. Gollin,[23] R. M. Hans,[23] E. Johnson,[23] I. Karliner,[23] M. A. Marsh,[23] C. Plager,[23] C. Sedlack,[23] M. Selen,[23] J. J. Thaler,[23] J. Williams,[23] K. W. Edwards,[24] and A. J. Sadoff[25]

(CLEO Collaboration)

[1]*University of Kansas, Lawrence, Kansas 66045*
[2]*University of Minnesota, Minneapolis, Minnesota 55455*
[3]*State University of New York at Albany, Albany, New York 12222*
[4]*The Ohio State University, Columbus, Ohio 43210*
[5]*University of Oklahoma, Norman, Oklahoma 73019*
[6]*University of Pittsburgh, Pittsburgh, Pennsylvania 15260*
[7]*Purdue University, West Lafayette, Indiana 47907*
[8]*University of Rochester, Rochester, New York 14627*
[9]*Southern Methodist University, Dallas, Texas 75275*
[10]*Syracuse University, Syracuse, New York 13244*
[11]*University of Texas, Austin, Texas 78712*
[12]*University of Texas–Pan American, Edinburg, Texas 78539*
[13]*Vanderbilt University, Nashville, Tennessee 37235*
[14]*Virginia Polytechnic Institute and State University, Blacksburg, Virginia 24061*
[15]*Wayne State University, Detroit, Michigan 48202*
[16]*California Institute of Technology, Pasadena, California 91125*
[17]*University of California, San Diego, La Jolla, California 92093*
[18]*University of California, Santa Barbara, California 93106*
[19]*Carnegie Mellon University, Pittsburgh, Pennsylvania 15213*
[20]*Cornell University, Ithaca, New York 14853*
[21]*University of Florida, Gainesville, Florida 32611*
[22]*Harvard University, Cambridge, Massachusetts 02138*
[23]*University of Illinois, Urbana-Champaign, Illinois 61801*
[24]*Carleton University, Ottawa, Ontario, Canada K1S 5B6*
and the Institute of Particle Physics, Canada
[25]*Ithaca College, Ithaca, New York 14850*

(Received 6 June 2001; published 11 December 2001)

We have searched for the two-body decay of the B meson to a light pseudoscalar meson $h = \pi^\pm$, $K^\pm, K_S^0$ and a massless neutral feebly interacting particle X^0 such as the familon, the Nambu-Goldstone boson associated with a spontaneously broken global family symmetry. We find no significant signal by analyzing a data sample containing 9.7×10^6 $B\bar{B}$ mesons collected with the CLEO detector at the Cornell Electron Storage Ring, and set 90% C.L. upper limits $\mathcal{B}(B^\pm \to h^\pm X^0) = 4.9 \times 10^{-5}$ and

$\mathcal{B}(B^0 \to K_S^0 X^0) = 5.3 \times 10^{-5}$. These limits correspond to a lower bound of approximately 10^8 GeV on the family symmetry breaking scale with vector coupling involving the third generation of quarks.

DOI: 10.1103/PhysRevLett.87.271801 PACS numbers: 14.80.Mz, 11.30.Qc, 13.25.Hw

The origin of family replication remains one of the major puzzles in particle physics. Why do we have three families of fermions, which are indistinguishable with respect to the strong and electroweak interactions? Neither the standard model (even incorporating the Higgs mechanism) nor its extension by various unification schemes in the framework of one family [SU(5), SO(10)] is able to provide a deep physical reason for the existence of the mass hierarchy among the generations and the weak mixing of quarks and leptons. In the absence of a concrete model, it is natural to assume that the underlying theory possesses a "horizontal" family symmetry which is spontaneously broken at some large energy scale. Among several possibilities, the most attractive is the assumption of a global (and continuous) flavor symmetry [1]. This symmetry, under some conditions [2], automatically induces the Peccei-Quinn symmetry and thus provides a solution for the strong *CP* problem [3]. The spontaneous symmetry breaking of a continuous global family symmetry implies the existence of neutral massless Nambu-Goldstone bosons [4], called familons, which can have flavor-conserving as well as flavor-changing couplings with the fermions [1].

The familon interaction at low energies can be described by the effective Lagrangian [5]

$$\Delta\mathcal{L}_f = \frac{1}{F}\,\partial_\mu f^a \bar{\psi}_i \gamma^\mu (g_V + g_A\gamma_5) T^a_{ij}\psi_j\,, \qquad (1)$$

where f^a are the familon fields, ψ are fermion fields, T^a are the generators of the broken family symmetry, g_V (g_A) is the (axial-)vector coupling, and F is the family symmetry breaking scale. The strength of the interaction is inversely proportional to the normalized family symmetry breaking scale $F_{ij} = F/\sqrt{(g_V T_{ij})^2 + (g_A T_{ij})^2}$, which can be constrained in a model-independent manner.

Upper limits on the rate of $K^+ \to \pi^+ X^0$ and $\mu^+ \to e^+(\gamma)X^0$ decays [6,7], where X^0 represents any neutral massless feebly interacting particle including the familon led to lower bounds on the normalized family symmetry breaking scale involving the first two generations $F^V_{sd} \gtrsim 10^{11}$ GeV [8] and $F_{\mu e} \gtrsim 10^9$ GeV in the hadronic and leptonic sector, respectively. In contrast, bounds on the flavor scale involving the third generation are less thoroughly studied experimentally, although some theoretical models suggest that the familon couples preferentially to the third generation [9]. The upper limits for $\tau \to \ell X^0$ ($\ell = e, \mu$) [10] led to a lower bound on the family symmetry breaking scale $F_{\tau\mu(e)} \gtrsim 10^6$ GeV in the leptonic sector, and no experimental bounds have been reported in the hadronic sector.

Familon couplings to the third generation are also of interest from a cosmological point of view. A massive unstable neutrino (typically the tau-neutrino) was proposed to decay into a lighter neutrino and a massless boson, such as a familon, in several cosmological scenarios related to big-bang nucleosynthesis [11], and large scale structure formation [12], in order to obtain a reasonable agreement between theory and observation. Since the process $\nu_\tau \to \nu_\ell f$ is related to the decay modes $\tau \to \ell f$ and $b \to q_d f$ ($q_d = d, s$) through $SU(2)_L$ and SU(5) unified gauge symmetries, respectively, searches for these decay modes can test the cosmological scenarios as well [5].

The decay of the b quark $b \to q_d f$ would lead to the decay $B \to hf$ ($h = \pi, K$) through vector coupling and $B \to Vf$ ($V = \rho, K^*$) through axial coupling, respectively. The latter decay modes are highly contaminated with combinatoric background due to the broad width of the ρ and K^* mesons. In contrast, the $B \to hf$ decays have the advantage that they exhibit a clean experimental signature with a single high energy charged meson or K_S^0 present in the final state, which can be detected with high efficiency, resulting in higher sensitivity for these decays. Hence, the purpose of this study is to search for the $B^\pm \to h^\pm X^0$ and $B^0 \to K_S^0 X^0$ decays, where X^0 could be any massless neutral particle that, like the familon, couples to ordinary matter very weakly. The lack of a signal allows us to obtain experimental constraint on the vector coupling of the familon to third generation hadrons for the first time. (The analysis is sensitive to new physics including any other massless feebly interacting neutral particles as well.)

The rate of the $B \to hf$ decay is related to the normalized family symmetry breaking scale $F^V_{bd(s)} = F/(g_V T_{bd(s)})$ through the formula [5]

$$\Gamma(B \to hf) = \frac{M_B^3}{16\pi}\left(1 - \frac{m_h^2}{M_B^2}\right)^3 \frac{|F_1(0)|^2}{(F^V_{bd(s)})^2}\,, \qquad (2)$$

where M_B, m_h are the masses of the mesons involved in the decay process and $F_1(q^2 = 0)$ is the weak transition $B \to h$ form factor at zero momentum transfer [13].

The data analyzed in this study were collected with the CLEO detector at the Cornell Electron Storage Ring (CESR), a symmetric e^+e^- collider. The components of the detector [14] most relevant to this analysis are the charged particle tracking system, the CsI electromagnetic calorimeter, and the muon detector. Trajectories of charged particles were reconstructed using a system of three concentric wire chambers covering 95% of the total solid angle, operating in an axial solenoidal magnetic field of 1.5 T. The main drift chamber also provided a measurement of the specific ionization loss (dE/dx) used for particle identification. Photons were detected by a CsI(Tl) electromagnetic calorimeter covering 95% of 4π. The muon chambers consisted of proportional counters embedded at various depths in the steel absorber. Approximately 2/3 of the data were collected with an upgraded detector, in which the innermost straw tube chamber was replaced with a three-layer, double-sided silicon vertex detector [15], and the gas in the main drift chamber was changed from an argon-ethane to a helium-propane mixture. These modifications led to an improved particle identification and momentum resolution.

The results in this Letter are based upon an integrated luminosity of 9.2 fb^{-1} of e^+e^- data corresponding to 9.7×10^6 $B\bar{B}$ meson pairs collected at the $\Upsilon(4S)$ resonance energy of 10.58 GeV ("on-resonance sample") and 4.6 fb^{-1} at 60 MeV below the $\Upsilon(4S)$ resonance ("off-resonance sample"). The study of the off-resonance sample enables us to statistically subtract the continuum ($e^+e^- \rightarrow q\bar{q}$, $q = u, d, c, s$) background contribution from the on-resonance sample. In order to study signal reconstruction efficiency and to optimize selection criteria, we generated Monte Carlo simulated samples with a GEANT-based [16] simulation of the CLEO detector response. Simulated data samples were processed in a similar manner as the data.

The experimental signature for the $B^\pm \rightarrow h^\pm X^0$ and $B^0 \rightarrow K_S^0 X^0$ decays is the escape of the neutral very feebly interacting particle X^0 from the detector without any trace and consequently leaving only its light meson partner to be observed. Because of the two-body decay structure, the meson partner is produced with a well defined momentum close to 2.64 GeV/c in the center of mass frame of the decaying B meson. However, in the lab frame its momentum is spread between 2.49–2.80 GeV/c due to the $\sim$0.32 GeV/c momentum of the B meson. Other detected particles and photons must be coming from the decay of the second B meson. Our analysis strategy to search for these decay modes is the following: (1) we select events with a well-identified light meson having a momentum in the expected range while (2) all remaining particles must be consistent with the decay of a second B meson, and (3) eliminate as much continuum background as possible and subtract the remaining continuum using off-resonance data. With the continuum subtracted, the high momentum candidates come from B decays. The dominant $b \rightarrow c$ decays do not contribute above 2.3 GeV/c. Rare $b \rightarrow u$ and $b \rightarrow s$ processes can produce high momentum mesons, but typically with other energetic particles which will spoil the reconstruction of the other B decay in the event. Decays such as $B^+ \rightarrow \pi^+ K_L^0$, $B \rightarrow K\nu\bar{\nu}$, and $B \rightarrow \tau\nu$ with $\tau \rightarrow h\nu$ will contribute at high momentum but are highly suppressed.

Candidates for the $\pi^\pm$ or $K^\pm$ meson partner of the familon ("meson candidate") were selected from well-reconstructed tracks originating near the e^+e^- interaction point (IP). Since charged π and K meson separation in the momentum range expected is difficult with the CLEO detector, we combined the charged B decay modes by requiring the charged meson candidate's dE/dx to be consistent with either the pion or the kaon hypothesis within 2.5 standard deviations (σ). We rejected electrons based on dE/dx and the ratio of the track momentum to the associated shower energy deposited in the CsI calorimeter. Muons were rejected based on the penetration depth in the steel absorber surrounding the detector. The K_S^0 candidates were reconstructed via their decay into $\pi^+\pi^-$ by requiring a decay vertex displacement from the IP and an invariant $\pi\pi$ mass within 10 MeV/c^2 of the known K_S^0 mass. We accepted meson candidates with momentum in the range $2.49 < p_{h^\pm} < 2.81$ GeV/c or $2.47 < p_{K_S^0} < 2.79$ GeV/c. This and the other selection criteria were optimized recursively by maximizing the signal significance, $S^2/(S + B)$, where S and B, the expected signal and background levels, were determined from Monte Carlo simulated samples assuming a signal branching fraction of 10^{-5}.

Since the remaining particles in the event must originate from the decay of the second B meson, we required that the beam constrained mass, $M(B) = \sqrt{E_{\mathrm{beam}}^2 - (\sum \mathbf{p}_i)^2}$, be close to the B meson mass and the energy difference, $\Delta E = \sum E_i - E_{\mathrm{beam}}$, be close to zero, where E_i and $\mathbf{p}_i$ are the energy and momentum of all detected particles (reconstructed tracks and photon shower candidates) in the event except for the meson candidate. The optimization of the selection criteria on the $M(B)$ and ΔE variables resulted in $M(B) > 5.245$ GeV/c^2 ($M(B) > 5.24$ GeV/c^2) and $-2.1 < \Delta E < 0.3$ GeV ($-3.0 < \Delta E < 0.4$ GeV) limits for the charged (neutral) B decay mode.

The main contribution to the background comes from continuum events. These events typically exhibit a two-jet structure and produce high momentum back-to-back tracks, while $B\bar{B}$ events tend to have a more isotropic decay structure, since the B mesons are produced nearly at rest ($P_B \approx 0.32$ GeV/c). We used the Fisher discriminant technique [17] to suppress the continuum background. The Fisher discriminant was formed as the linear combination of 14 shape variables: 9 momentum flow variables (the sum of the momentum of all detected particles in 10° angular bins around the direction of the meson candidate); the angle between the momentum of the other B meson reconstructed from the rest of the event and the e^+e^- collision ("beam") axis; the angle between the momentum of the meson candidate and the beam axis; the second order normalized Fox-Wolfram moment [18]; the angle between the momentum of the meson candidate and the thrust axis of the rest of the event; and the maximum opening angle of the cone opposite to the momentum of the meson candidate, in which no other charged track, π^0 or K_S^0, was detected. The combination coefficients were chosen to maximize the separation between the simulated signal and continuum background samples.

The distribution of the Fisher discriminant used in the analysis is shown for simulated events and off-resonance data on Fig. 1. The agreement between simulated continuum and off-resonance events is very good. We selected candidate events with a Fisher discriminant less than 0.29

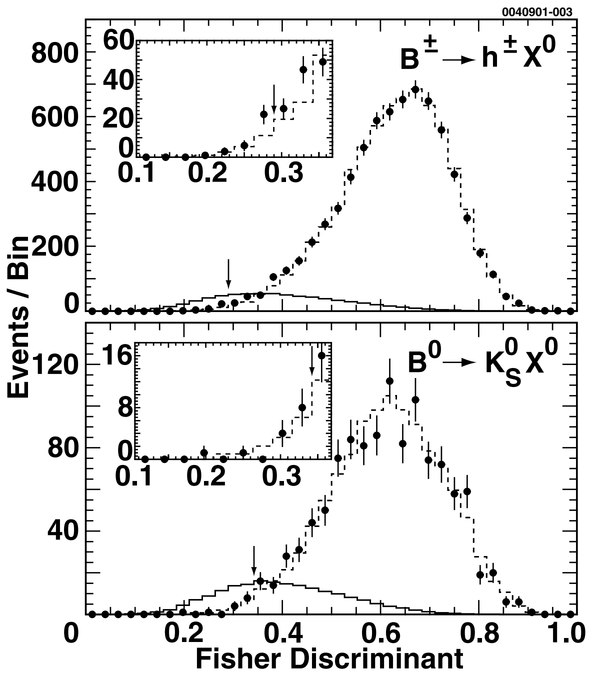

FIG. 1. Distribution of the Fisher discriminant for simulated signal (solid) and continuum (dashed) as well as off-resonance data (points) samples. The histograms are normalized to the statistics of the off-resonance data. The signal histograms are plotted assuming a branching fraction of $\mathcal{B}(B^\pm \to h^\pm X^0) = 50 \times 10^{-5}$ and $\mathcal{B}(B^0 \to K_S^0 X^0) = 20 \times 10^{-5}$. The vertical arrow represents the optimum selection value below which events were accepted. Insets show the tail of the continuum distributions around the cut value.

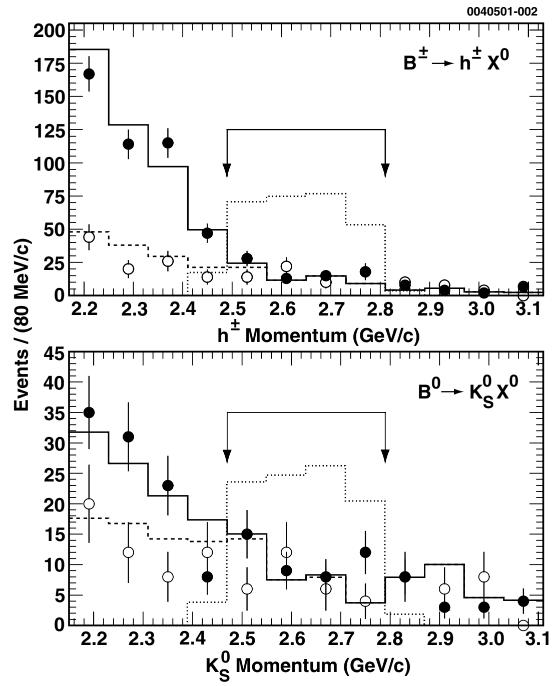

FIG. 2. Momentum distribution of the meson candidates. Filled and empty dots represent the on-resonance and the normalized off-resonance data, respectively. Solid histogram shows the prediction from $e^+e^- \to q\bar{q}$ plus $b \to c$ simulations while the dashed histogram shows the distribution from $e^+e^- \to q\bar{q}$ only. These histograms are normalized to the statistics of our data sample. Simulated signal events are shown by the dotted histogram assuming that $\mathcal{B}(B^\pm \to h^\pm X^0) = 30 \times 10^{-5}$ and $\mathcal{B}(B^0 \to K_S^0 X^0) = 12 \times 10^{-5}$. The accepted signal region is indicated by the arrows.

in case of the charged B decay mode and less than 0.34 for the neutral B decay mode.

The overall signal selection efficiency is 7.2% for $B^\pm \to h^\pm X^0$ and 6.6% for the $B^0 \to K_S^0 X^0$ events. The systematic error on the efficiency is 13% (18%) for the charged (neutral) B decay mode. The contributions to this error are due to the uncertainties in the tracking efficiency, 2% (4%); the momentum selection, 1% (1%); $M(B)$ and ΔE selection, 6% (6%); Fisher discriminant restriction, 11% (16%); and limited Monte Carlo statistics, 1% (1%).

Figure 2 shows the momentum distribution of the meson candidate for on-resonance and off-resonance events along with the distributions for simulated events after all selection criteria except the tight momentum restriction on the meson candidate were applied. The number of on-resonance (off-resonance) events in the selected momentum range is 74 (32) in case of the $B^\pm \to h^\pm X^0$ and 44 (14) in case of the $B^0 \to K_S^0 X^0$ analysis. The study of the background from $b \to c$, and other rare $b \to u$ and $b \to s$ decays using simulated data samples showed these to be negligible with the largest contribution of less than five events coming from $B^+ \to \pi^+ K_L^0$ decay.

We calculated the branching fraction based on

$$\mathcal{B} = \frac{N_{\rm on} - RN_{\rm off}}{\varepsilon N_B}, \quad (3)$$

where $N_{\rm on}$ ($N_{\rm off}$) is the number of observed events in the on- (off-) resonance sample after all cuts are applied; $R = 2.00 \pm 0.04$ is the normalization coefficient between the two samples; ε is the signal selection efficiency; and $N_B = (9.7 \pm 0.2) \times 10^6$ is the total number of charged (neutral) B mesons in the data sample, assuming equal production of charged and neutral B meson pairs from the $\Upsilon(4S)$ [19]. We find $\mathcal{B}(B^\pm \to h^\pm X^0) = (1.4 \pm 2.1) \times 10^{-5}$ and $\mathcal{B}(B^0 \to K_S^0 X^0) = (2.5 \pm 1.7) \times 10^{-5}$. The error in the branching fraction is dominated by the statistical error in $N_{\rm on}$ and $N_{\rm off}$. We derived a 90% confidence level upper limit based on the frequentist approach applied for Gaussian data close to a physical boundary [20]: $\mathcal{B}(B^\pm \to h^\pm X^0) < 4.9 \times 10^{-5}$ and $\mathcal{B}(B^0 \to K_S^0 X^0) < 5.3 \times 10^{-5}$.

The upper limits can be converted into a lower bound on the normalized family symmetry breaking scale, $F_{bs(d)}^V$, with vectorlike coupling between the familon and the quarks using Eq. (2). To do so we take the form factor $F_1(q^2 = 0)$ to be 0.25 from [13]. The upper limit on the branching fraction of $B^0 \to K_S^0 X^0$ gives $F_{bs}^V > 6.4 \times 10^7$ GeV. The other limit gives a slightly better bound of $F_{bs(d)}^V > 1.3 \times 10^8$ GeV with the assumption that the familon couples to the d and s quark with approximately the same strength ($F_{bs} = F_{bd}$).

In conclusion, we performed a search for the decays $B^{\pm} \rightarrow h^{\pm}X^0$ and $B^0 \rightarrow K_S^0 X^0$, setting upper limits for the branching fractions at 4.9×10^{-5} and 5.3×10^{-5}, respectively. These limits constrain new physics leading to two-body B decays involving any massless neutral feebly interacting particle X^0. Applying the limit to the case where X^0 is a familon, we obtain the first lower bound on the family symmetry breaking scale $F^V_{bs(d)}$ involving the third generation of quarks at 10^8 GeV.

We gratefully acknowledge the effort of the CESR staff in providing us with excellent luminosity and running conditions. This work was supported by the National Science Foundation, the U.S. Department of Energy, the Research Corporation, the Natural Sciences and Engineering Research Council of Canada, and the Texas Advanced Research Program.

[1] D. B. Reiss, Phys. Lett. **115B**, 217 (1982); F. Wilczek, Phys. Rev. Lett. **49**, 1549 (1982); G. B. Gelmini, S. Nussinov, and T. Yanagida, Nucl. Phys. **B219**, 31 (1983).
[2] D. Chang and G. Senjanović, Phys. Lett. B **188**, 231 (1987).
[3] R. D. Peccei and H. R. Quinn, Phys. Rev. Lett. **38**, 1440 (1977); Phys. Rev. D **16**, 1791 (1977).
[4] J. Goldstone, Nuovo Cimento **19**, 154 (1961); J. Goldstone, A. Salam, and S. Weinberg, Phys. Rev. **127**, 965 (1962).
[5] J. L. Feng, T. Moroi, H. Murayama, and E. Schnapka, Phys. Rev. D **57**, 5875 (1998).
[6] E787 Collaboration, S. Adler *et al.,* Phys. Rev. Lett. **79**, 2204 (1997).
[7] A. Jodidio *et al.,* Phys. Rev. D **34**, 1967 (1986); R. D. Bolton *et al.,* Phys. Rev. D **38**, 2077 (1988).
[8] The limit on $\mathcal{B}(K \rightarrow \pi X^0)$ places a bound on the vectorial familon coupling only, which is inversely proportional to $F^V_{ij} = F/(g_V T_{ij})$ [5]; the axial coupling is unconstrained since the matrix element $\langle \pi(p') | \bar{d} \gamma_\mu \gamma_5 s | K(p) \rangle \equiv 0$.
[9] Z. Berezhiani and M. Kholopov, Z. Phys. C **49**, 73 (1991).
[10] ARGUS Collaboration, H. Albrecht *et al.,* Z. Phys. C **68**, 25 (1995).
[11] S. Hannestad, Phys. Rev. D **57**, 2213 (1998).
[12] M. White, G. Gelmini, and J. Silk, Phys. Rev. D **51**, 2669 (1995).
[13] P. Colangelo, F. De Fazio, P. Santorelli, and E. Scrimieri, Phys. Lett. B **395**, 339 (1997).
[14] CLEO Collaboration, Y. Kubota *et al.,* Nucl. Instrum. Methods Phys. Res., Sect. A **320**, 66 (1992).
[15] T. Hill, Nucl. Instrum. Methods Phys. Res., Sect. A **418**, 32 (1998).
[16] R. Brun *et al.,* GEANT 3.15, CERN Report No. DD/EE/84-1, 1987.
[17] CLEO Collaboration, D. M. Asner *et al.,* Phys. Rev. D **53**, 1039 (1996).
[18] G. C. Fox and S. Wolfram, Phys. Rev. Lett. **41**, 1581 (1978).
[19] CLEO Collaboration, J. P. Alexander *et al.,* Phys. Rev. Lett. **86**, 2737 (2001).
[20] Particle Data Group, D. E. Groom *et al.,* Eur. Phys. J. C **15**, 1 (2000); G. J. Feldman and R. D. Cousins, Phys. Rev. D **57**, 3873 (1998).